RADIOMETRIC QUALITY AND DSM GENERATION ANALYSIS OF CARTOSAT-1 STEREO IMAGERY

M. Crespi[a], L. De Vendictis[c], D. Poli[b], K. Wolff[b], G. Colosimo[a], A. Gruen[b], F. Volpe[c]

[a]DITS – Area di Geodesia e Geomatica – Sapienza Università di Roma – via Eudossiana 18 – Rome, Italy - mattia.crespi@uniroma1.it
[b]Institute of Geodesy and Photogrammetry, ETH Zurich, Wolfgang-Pauli-Strasse 15 8093 Zurich, Switzerland - <armin.gruen,daniela.poli,kirsten.wolff>@geod.baug.ethz.ch
[c]Eurimage S.p.A. – via D'Onofrio 212 – Rome, Italy - <volpe,l.devendictis>@eurimage.com

Commission I, SS-11

KEY WORDS: Accuracy, DEM/DTM, High resolution, Matching, Orientation, Radiometric Quality, Satellite,

ABSTRACT:

CARTOSAT-1, launched in May 2005, is equipped with two cameras, Aft and Fore, tilted along-track by -5° and +26° respectively, allowing the acquisition of stereo data with a geometrical resolution of 2.5 m. The Institute "Area di Geodesia e Geomatica" at Sapienza Università di Roma, Eurimage S.p.A. and the Institute of Geodesy and Photogrammetry, ETH Zurich participated in the ISPRS-ISRO Cartosat-1 Scientific Assessment Programme (C-SAP), in order to investigate the generation of Digital Surface Models (DSMs) from Cartosat-1 stereo scenes. This paper follows up on the previous work done by the Institutes and shows the analysis of a new standard stereopair belonging to the additional test field TS-Castelgandolfo, acquired on 18th July 2006 over the area of Castelgandolfo, Rome, Italy (30 x 30 km^2). The images are processed, in order to test both the image quality and the potential for DSM generation, following the procedures already established. The results obtained in all steps of the investigation, particularly those related to image quality, the orientation with different models and software and the effectiveness of image filtering for enhancing the DSM generation are presented and discussed.

1 INTRODUCTION

CARTOSAT-1, launched in May 2005, is equipped with two cameras, Aft and Fore, tilted along track by -5° and +26° respectively, allowing the acquisition of stereo data with a geometrical resolution of 2.5 (Krishnaswamy, 2002).
The Institute "Area di Geodesia e Geomatica" at Sapienza Università di Roma, Eurimage S.p.A. and the Institute of Geodesy and Photogrammetry, ETH Zurich participated in the ISPRS-ISRO Cartosat-1 Scientific Assessment Programme (C-SAP), in order to investigate the generation of Digital Surface Models (DSMs) from Cartosat-1 stereo scenes (Kocaman et al., 2008, Baltsavias et al., 2007, Barbato et al., 2007).

This paper follows up on the work done with the stereopair belonging to the test field called TS-6, acquired on 8th June 2005 over the city of Rome, Italy, which was a very preliminary (just about one month after the launch) non-standard acquisition (7.5 x 30 km^2), since only a short part of the CCD array (3000 pixels vs. a total of 12000) was active. The results of this part of the work were presented in (Barbato et al., 2007). Now a new standard stereopair belonging to the additional test field TS-Castelgandolfo, acquired on 18th July 2006 over the area of Castelgandolfo, Rome, Italy (30 x 30 km^2) is processed in order to test both the image quality and the potential for DSM generation, following the procedures already established.

The results obtained in all steps of the investigation, particularly those related to image quality, orientation with different models and software, effectiveness of image filtering for enhancing the DSM generation and the potential of DSM generation itself are presented and discussed.

2 DATA DESCRIPTION

The dataset TS-Castelgandolfo of C-SAP contains a stereopair from the Cartosat-1 satellite with corresponding metadata files, the monographs of 25 ground points and a Digital Surface Model (DSM) derived from aerial images.

The two stereo images were acquired on 18th July, 2006 in the morning, over Castelgandolfo and Colli Albani, a volcanic area Southeast of Rome. The scenes have a time interval of 54 sec and an in-track overlap of almost 90%. Each image has the size 12'000 pixel x 12'000 pixels, with a ground resolution of 2.5 m. The area is characterized by the presence of volcanoes, crater lakes and isolated villages. The elevation ranges between 50 m and 1000 m.

The scenes were acquired in panchromatic mode with mean attitude angles (roll, pitch, yaw) of (-11.3, 0.0, 2.49) degrees respectively. The metadata files contain information on the acquisition time, scene location, mean attitude angles, sensor geometry (detectors looking angles) and satellite orbit. The state vectors of the sensor (position and velocity) during the acquisition were not available.

In addition to the satellite images, a block of 31 aerial images, arranged in 5 strips and covering an area of about 85 km^2 in the central part of the images from Cartosat-1, are available. They were used to generate a reference DSM. The aerial block was acquired during 2003 with a Wild RC-20 camera (lens type 15/4 UAGA-F, focal length 152.18 mm) at an average scale of 1:15000 with an along-track overlap of 70 % and a cross-track overlap of 20 %. For block orientation, 26 well distributed

GCPs were collected by a RTK GPS survey assisted by the RESNAP-GPS permanent network of the Lazio Region, (managed by the Area di Geodesia e Geomatica - Sapienza Università di Roma) with a 3D accuracy of 15 cm. The block triangulation was performed both by Leica Photogrammetric Suite (LPS) 9.1 and BLUH software. Finally, the image matching and the DSM generation at 2m grid spacing were performed using LPS.
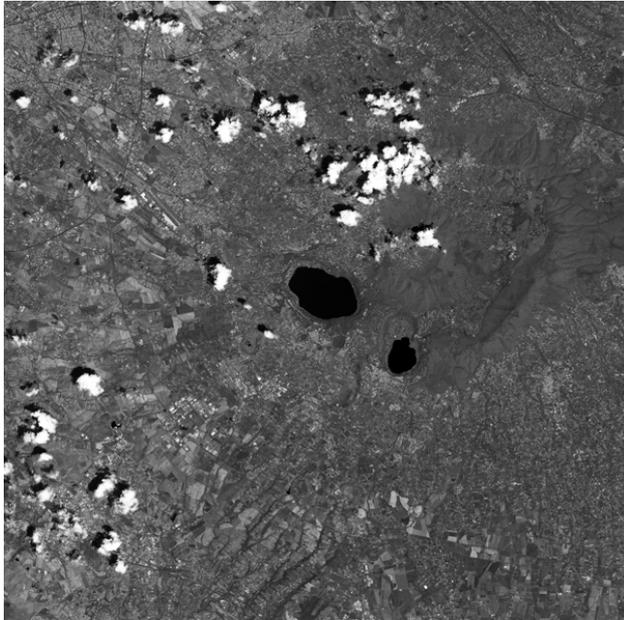

Figure 1. Overview of Cartosat-1 Band A. The image size is 12'000 x 12'000 pixels. Some crater lakes are visible.

3   RADIOMETRY ANALYSIS

Within the chain from image sensing to the final value-added product the quality of the images plays a crucial role. Image quality is defined by several parameters, as the radiometric resolution and its accuracy, represented by the noise level, and the geometrical resolution and sharpness, described by the Modulation Transfer Function (MTF). In the next sections these parameters are investigated for the scenes used in this work. Other radiometric problems, like vertical striping effects, have not been observed at a significant level.

3.1   Image noise analysis

The image noise characteristics are important for the image matching process in the DSM generation.

Nowadays, most of the linear array sensors have the ability to provide more than 8-bit/pixel digital images. The Cartosat-1 sensor provides images with 10 bit/pixel, that means 1024 available grey levels, but 99% of the original pixel values vary between 0 and 255.

A preliminary analysis was carried out to investigate the noise dependency on image intensity. According to the method proposed in (Baltsavias et al., 2001), and (Zhang, 2005) the noise characteristics of the stereopair were analyzed using the standard deviations of the grey values in non-homogeneous image regions, that allow to evaluate the noise variations as a function of intensity.

In order to evaluate the noise level, a window (3x3 pixels) is moved within the area by 3-pixel steps in both directions and the standard deviation and the mean grey value are calculated for each window. The grey level range is divided in bins, and the standard deviations are assigned to a bin according to the mean grey value of each window. In each bin the noise is estimated as the mean of the 5% smallest standard deviations, under the hypothesis that the variability within the window should represent just the noise and not the different texture. The results reported in `Figure 2` indicate that the noise is intensity dependent showing smaller noise values for the bins of low grey levels than for the high grey ones. This is a well known effect, also present in digital aerial images.
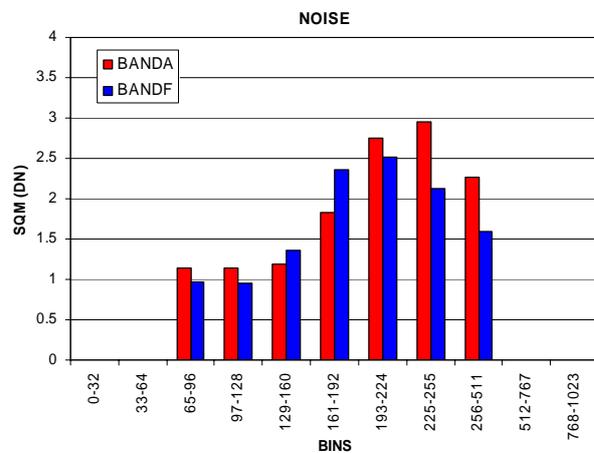

Figure 2. Cartosat-1 noise level estimation.

3.2   Modulation Transfer Function (MTF) analysis

The image sharpness was addressed through the analysis of its Modulation Transfer Function (MTF) that represents, in the spatial frequency domain and for a given direction, the image spatial resolution. The transfer function of the system can be obtained considering the response (Edge Spread Function – ESF) of the optical system to an ideal edge (rectangular pulse). Multiple methods have been proposed for determining the MTF of remote sensing systems in-orbit. Most of the procedures use specific artificial or natural targets on the ground for estimating the Edge Spread Function (ESF). Through the first derivative of the ESF it is possible to obtain the Line Spread Function (LSF), whose Fourier Transform provides the Modulation Transfer Function (MTF) (`Figure 3`).
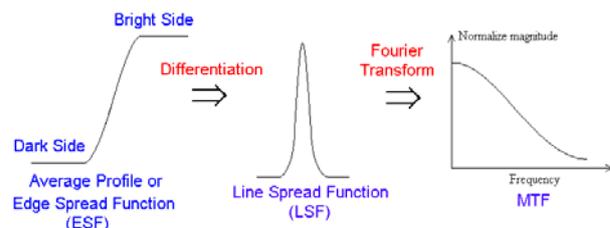

Figure 3. Edge MTF estimation method.

In this work we estimated the MTF for Cartosat-1 images starting from the "edge method" proposed by (Choi, 2002), then recently revised by (De Vendictis, 2008).

The initial task of the edge method algorithm is the identification of suited pseudo-rectilinear target edges, approximately oriented along and across scan direction, that show a blurred line edge between two relatively uniform regions with different intensities. Assuming that the chosen edges represent a straight line, the alignment of all edge locations is done with a least squares error fitting technique. The edge profiles, which are centred at each edge pixel and have the direction perpendicular to the edge, are interpolated with cubic spline functions and averaged to obtain a curve that represents the response of the sensor to the input signal. The ESF is obtained interpolating this curve with an analytic function that reduces the noise (De Vendictis, 2008). The ESF is then differentiated to obtain the LSF and the LSF is Fourier-transformed and normalized to obtain the corresponding MTF.

The computed MTF is scaled in the frequency axis in order to represent the calculated MTF in terms of the Nyquist frequency of the image. In addition, the Full Width at Half Maximum (FWHM) value is computed.

20 Edges	Along track direction		Cross track direction	
	MTF at Nyquist	FWHM (pixels)	MTF at Nyquist	FWHM (pixels)
BANDA (-5°)	0.26	1.45	0.16	1.75
BANDF (+26°)	0.15	1.87	0.06	2.49

Table 1. MTF and FWHM estimation results

As can be seen from `Table 1`, the MTF values for along-track direction are always larger than those for cross-track direction and the BANDA has a remarkable better quality than BANDF, both with respect to FWHM and MTF.

GCPs	ERDAS – RPC Order 1			SAT-PP - RPC Order 1			PCI – Rigorous model		
	E (m)	N (m)	H (m)	E (m)	N (m)	H (m)	E (m)	N (m)	H (m)
4	1.53	1.52	1.69	1.32	1.45	1.29	-	-	-
6	1.56	1.42	1.70	1.31	1.32	1.25	4.31	2.60	1.66
9	1.48	1.56	1.64	1.17	1.38	1.17	0.98	1.34	1.20

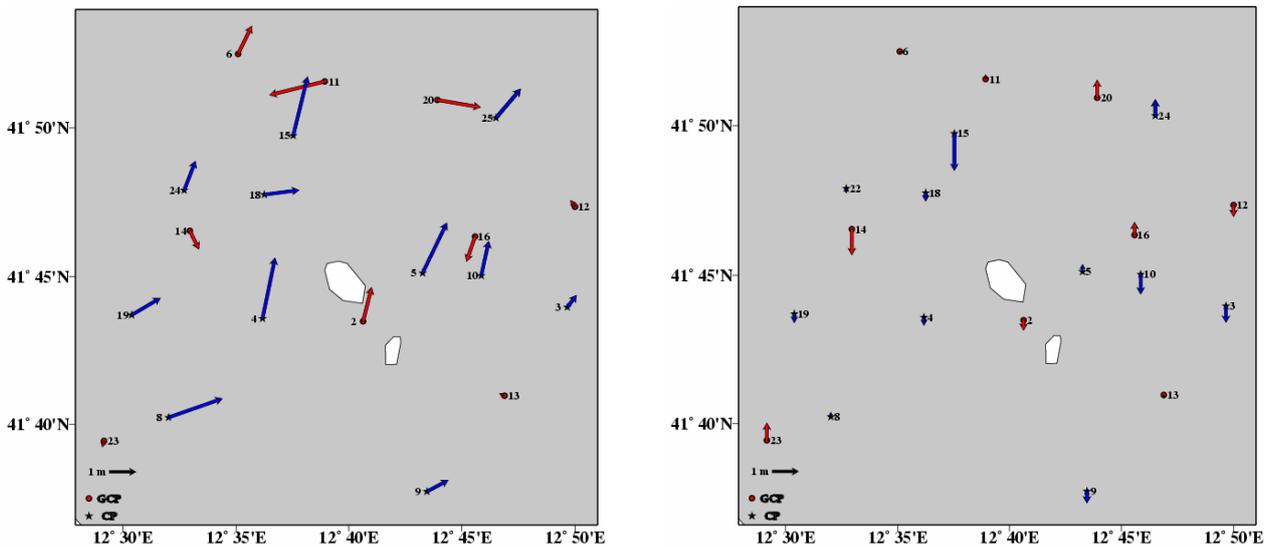Table 2. RMSEs (in meters) at check points after image orientation using three different approaches

Figure 4. Distribution of residuals in planimetry (left) and height (right) at GCPs and CPs after orientation in PCI with a rigorous model and 9 GCPs.

4   IMAGE ORIENTATION

For the image orientation two different approaches were adopted: the rigorous model, implemented in the PCI-OrthoEngine software, and the Rational Function Model (RPC) with 1st order correction, included in the ERDAS Imagine and in the SAT-PP (Satellite Image Precision Processing) software, developed at the ETH Zurich. According to our experiences from previous tests on Cartosat-1 stereopair orientation

(Barbato et al., 2007), the RPC model with no correction is not sufficient. The stereopair was oriented using 4, 6 and 9 Ground Control Points (GCPs), and the remaining points were kept as Check Points (CPs). For each number of GCPs an optimal distribution was used. The results were evaluated in terms of RMSE on the CPs. In order to detect blunders, the orientation was performed using all points as GCPs. Among the available 25 points, 20 points were kept for the orientation. The results obtained from image orientation, summarized in Table 2, show

sub-pixel accuracy in all directions. SAT-PP performs better than ERDAS (differences up to 1/5 of the ground pixel size), while the rigorous model of PCI needs more GCPs in order to perform well. The residual distributions of Figure 4 after orientation with PCI rigorous model show some inconsistencies. There is a clear systematic deformation visible in the planimetric residuals of the CPs, which is however not present in the GCPs. Therefore the results of the rigorous model should be analysed more in detail in terms of statistical behaviour of each unknown parameter. In particular self-calibration and external orientation modelling should be studied more in detail. Unfortunately this is not possible with the PCI software. The rigorous models developed at ETH Zurich (Poli, 2005, Kocaman and Gruen, 2007) and Sapienza Università di Roma (Crespi et al., 2007) will be extended in order to process Cartosat-1 scenes and complete the investigations in this respect. In addition more tests are required for the analysis of GCPs distribution, which seems to have an influence on the accuracy of Cartosat-1 stereoscenes, especially in planimetry (Kocaman et al., 2008). During the investigations the accuracy assessment will be performed using the Leave-One-Out method too, as proposed in Brovelli et al., (2008). In fact the leave-one-out method is a well known statistical estimation technique currently applied in different fields such as machine learning, bioinformatics and generally in any other field requiring an evaluation of the performance of a learning algorithm (e.g. in geostatistics) and can give a good contribution for accuracy assessment, avoiding to draw conclusions which are constrained to a particular set of CPs.

5   DSM GENERATION

The image matching was carried out independently with the software packages PCI-Orthoengine and SAT-PP, since they contain different matching strategies. PCI-Orthoengine uses crosscorrelation, whereas SAT-PP uses a multi-image matching approach especially designed for Linear Array sensors, based on the extraction of three kinds of features (feature points, grid points and edges), as explained in (Baltsavias et al, 2006, Gruen and Wolff, 2007)

Clouds are not part of the requested surface model. Therefore they were masked out by manual measurements in the images.The same was done for water surfaces, because they are also disturbing elements for the image matcher.

Taking into account that the different radiometry between the two images, due to the variations in the sensor view angles, may influence the matching results, the Cartosat-1 images were filtered to enhance the edges and then to reduce the radiometric errors. The images used for DSM generation in PCI have been radiometrically processed with a) a smoothing moving average filter to reduce the high frequency noise, and then b) a Sobel filter, that transformed the images into gradient maps. In case of SAT-PP, the matching algorithm applies a Wallis filter internally. After matching the images, from the 2D coordinates of the homologous points the corresponding 3D point clouds were generated using the corresponding orientation parameters previously estimated, and interpolated to generate a 5m grid surface model. In SAT-PP masks were manually measured in order to exclude clouds and water surfaces (i.e. lakes) from the DSM computation.
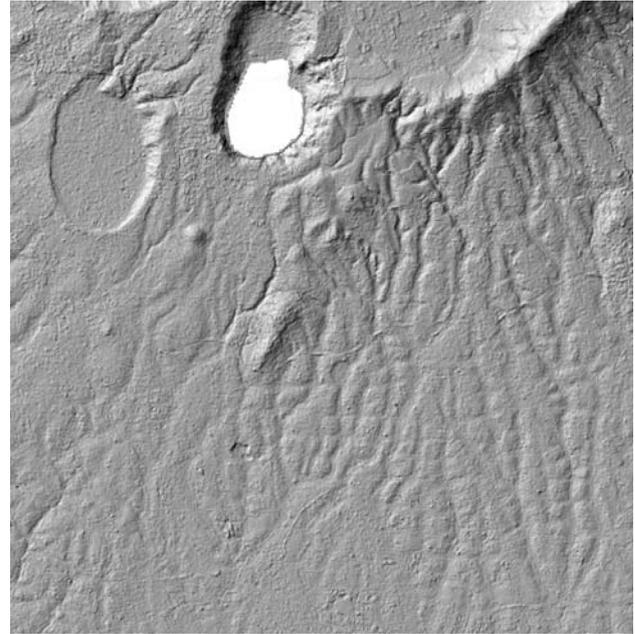

Figure 5. Zoom into the SAT-PP DSM, visualized in shading mode. The white area is part of the mask.

6   ACCURACY ANALYSIS

At this stage, the corresponding DSMs were interpolated and compared to the reference DSM over an area of only 2km x 2km with urban and open zones and free from clouds (Figure 6).
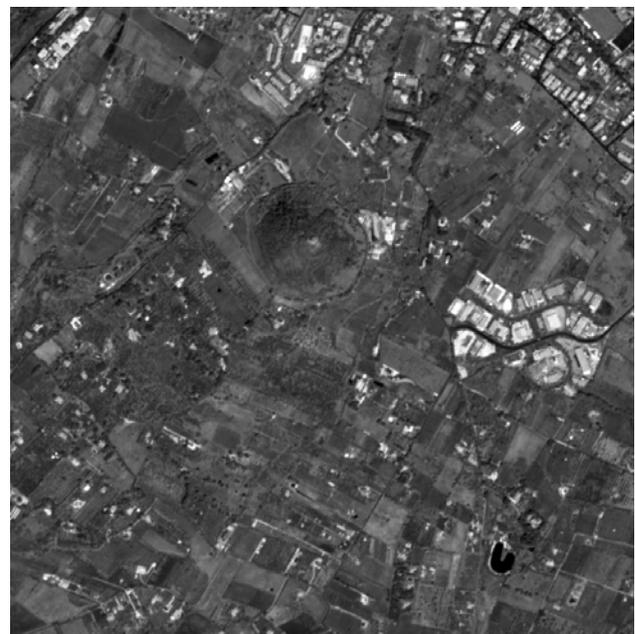

Figure 6. Area used for DSM comparison (BAND A).

The 3D differences were computed through a co-registration with the LS3D (Least Squares 3D Surface Matching) software, developed at ETH Zurich, which includes an algorithm for least squares matching of overlapping 3D surfaces (Akca and Gruen,

2005). It is crucial to perform a full 3D comparison, because a 2.5D analysis (generally done by most of the GIS commercial software) could overestimate the differences between two surfaces representing the same object. In fact, comparing heights instead of surface normals causes errors especially in cases where even small horizontal errors (georeferencing discrepancies or errors in point measurements) may lead to big height deviations, introducing methodological errors into the testing procedure.

The DSMs generated with SAT-PP and PCI were co-registered to the reference DSM and between themselves. The shift values are reported in Table 3, 2nd to 4th columns. With respect to the reference data, the SAT-PP DSM shows a shift in East direction of about 0.5 pixels and a larger shift (about 1.4 ground pixels) in North direction, while PCI DSM has a shift of 1.3-1.5 ground pixels in planimetry. For both surfaces, the shift in Z direction is not significant. This results in an overall shift between SAT-PP and PCI DSM of 3 ground pixels in North direction, which

is the satellite flight direction. This issue will be investigated in the future.

After transforming the surfaces to a common system using the estimated shift parameters, the 3D residuals have been computed. From Figure 7 we see that the residuals are normally distributed with null bias. In Table 3 the mean values and RMSE of the residuals in Euclidean direction and in the 3 components East, North and height, are reported (5th to 9th columns). The residuals in planimetry between the generated DSMs and the reference DSM are almost the same, while in height large differences exist. Figure 8 shows that the largest errors are located in urban areas. We suppose that some differences in height are due to surface changes between the acquisition time of the Cartosat-1 scenes and the aerial images used for the reference DSM generation. If we analyse the residual distribution between SAT-PP and PCI DSM (Figure 9), we see that after co-registration the two surface models fit quite well (about half a pixel RSME). Again, the largest values are present in height.
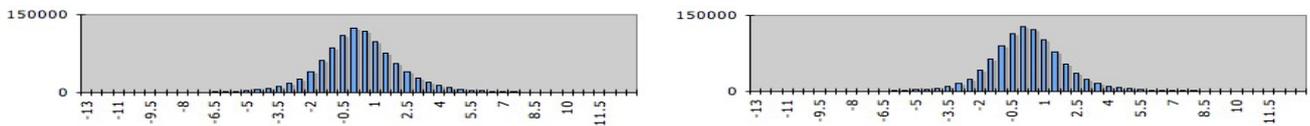

Figure 7. Histograms of residuals between reference DSM and Sat-PP DSM (left) and PCI DSM (right) after coregistration.

DEM	Shift (m)			Residuals (m)				
	E	N	H	Mean 3D	RMSE 3D	RMSE E	RMSE N	RMSE H
Ref vs. SAT-PP	1.52	-3.37	-0.20	0.02	2.07	0.39	0.37	2.00
Ref vs. PCI	3.16	3.55	0.59	0.02	2.02	0.41	0.44	1.94
SAT-PP vs. PCI	2.10	7.67	0.86	0.00	1.39	0.30	0.30	1.32

Table 3. 3D comparison between PCI, SAT-PP and reference DSM for area 1: shifts between DSMs, residuals after co-registration. The first surface has been used as search, the second as template.
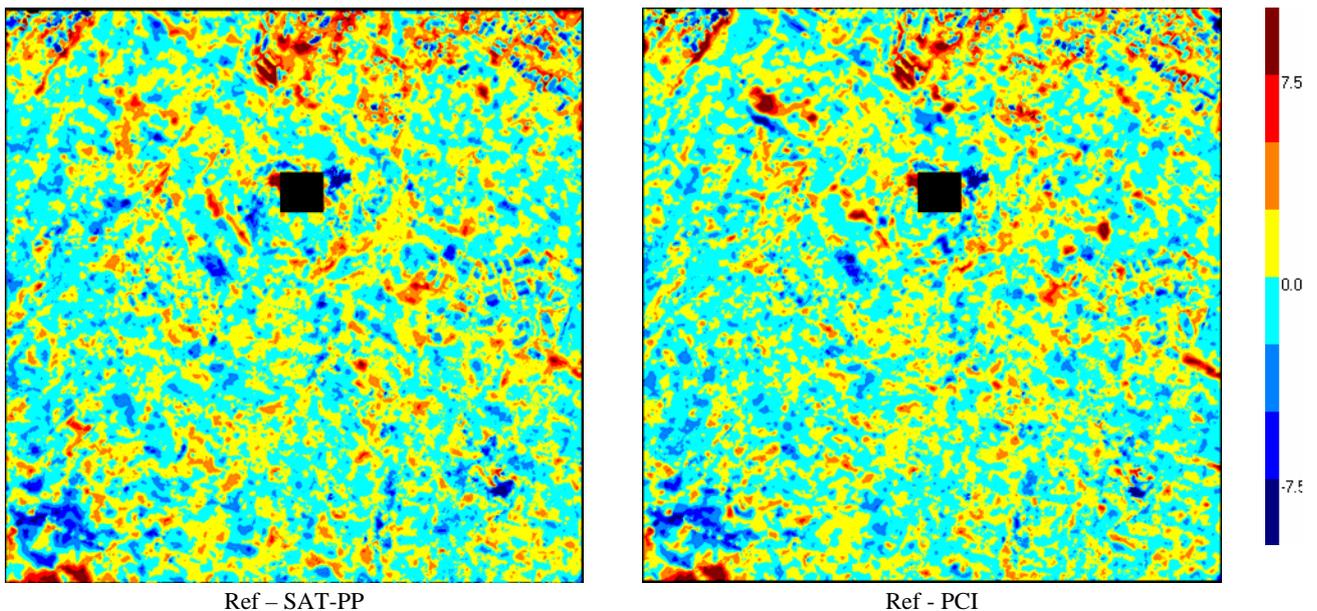

Ref – SAT-PP

Ref - PCI

Figure 8. Residual distribution (in meters) after co-registration between SAT-PP and PCI DSMs (template surfaces) with respect to the reference DSM (search surface) in Euclidean direction. The black area is excluded from the analysis due to a gap in the reference surface.

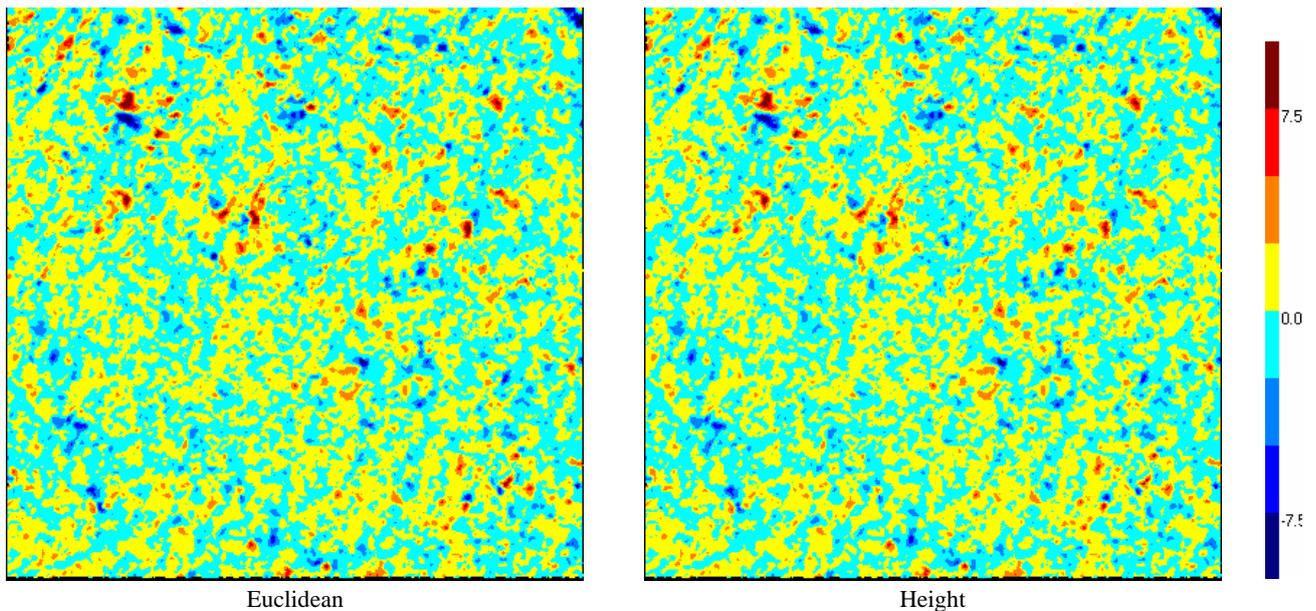| Euclidean	Height

Figure 9. Residual distribution after coregistration between SAT-PP and PCI DSMs in Euclidean direction and in height.

7   CONCLUSIONS AND PROSPECTS

A Cartosat-1 stereopair belonging to test field TS-Castelgandolfo was processed in order to test image quality, orientation with different models and software, effectiveness of image filtering for enhancing the DSM generation and potential for DSM generation itself.

The main results can be summarized as:
- the noise is intensity dependent, with smaller noise values at low grey levels
- the MTF values for along-track direction are always larger (and thus better) than those for cross-track direction and the BANDA has a remarkable better quality than BANDF
- the image orientations show sub-pixel accuracies in all directions; the rigorous model in PCI software required more GCPs than the RPC correction model (based on affine transformation) to perform well
- two different preprocessing strategies were performed: a smoothing moving average filter plus the Sobel filter, that transformed the images into gradient maps for PCI; Wallis filter for SAT-PP; both strategies were found effective for the subsequent DSM generation, which led to similar results with an overall 3D and vertical accuracy at the level of 2m. For future investigations, some of the following points could be addressed:
- additional tests about the noise level of BANDA vs. BANDF have to be performed
- additional tests using the Leave-One-Out method have to be carried out to give general recommendations; moreover, the statistical significance of the parameters estimated within a rigorous model should be analyzed
- the dependence of the DSM accuracy on different land cover areas has to be analyzed and the overall shift between SAT-PP and PCI DSM of about 3 ground pixels in North direction, which is the satellite flight direction, has to be investigated.

REFERENCES

Akca, D., Gruen, A., 2005. Least squares 3D surface and curve matching. ISPRS Journal of Photogrammetry and Remote Sensing 2005, Vol. 59 (3), pp.151-174.

Barbato, F., Crespi, M., De Vendictis, L., Iannucci, G., Onori, R., Poli, D., Volpe, F., Wang, X., 2007. Cartosat-1 stereo imagery: potentialities about orientation, DSM extraction and orthorectification. Proceedings of 27th EARSeL Symposium "Geoinformation in Europe", 4-7 June 2007, Bolzano, Italy.

Baltsavias, E. P., Pateraki, M., Zhang, L. 2001. Radiometric and Geometric Evaluation of IKONOS Geo Images and Their Use for 3D Building Modeling. Joint ISPRS Workshop on High Resolution Mapping from Space 2001, Hannover, Germany, 19-21 September (on CD-ROM).

Baltsavias, E., Zhang, L., Eisenbeiss, H., 2006. DSM Generation and Interior Orientation Determination of IKONOS Images Using a Testfield in Switzerland. Photogrammetrie, Fernerkundung, Geoinformation, (1), pp. 41-54.

Baltsavias E., Kocaman S., Akca D., Wolff K., 2007. Geometric and Radiometric Investigations of Cartosat-1 Data. ISPRS Hannover Workshop 2007, "High Resolution Earth Imaging for Geospatial Information", Hannover, Germany, May 29- June 1 (proceedings on CD-ROM).

Brovelli, M. A., Crespi, M., Fratarcangeli, F., Giannone, F., Realini, E., 2008. Accuracy assessment of high resolution satellite imagery orientation by leave-one-out method. *ISPRS J. Photogram . Rem. Sens.* (in press).

Choi, T. 2002. IKONOS Satellite on Orbit Modulation Transfer Function (MTF) Measurement using Edge and Pulse Method. Master Thesis, South Dakota State University.

Crespi, M., Fratarcangeli, F., Giannone, F., Pieralice, F., 2007. SISAR: a Rigorous Orientation Model for Synchronous and Asynchronous Pushbroom Sensors Imagery. ISPRS Hannover Workshop 2007, "High Resolution Earth Imaging for Geospatial Information", Hannover, Germany, May 29- June 1 (proceedings on CD-ROM).

De Vendictis, L., 2008. Quality assessment and enhancement of High Resolution Satellite Imagery for Digital Surface Model extraction. PhD Thesis, Area di Geodesia e Geomatica Dipartimento di Idraulica Trasporti e Strade, Sapienza Università di Roma.

Gruen, A., Wolff, K., 2007. DSM Generation with ALOS/PRISM Data Using SAT-PP. IEEE International Geoscience and Remote Sensing Symposium (IGARSS) 2007, July 23 -27 (proceedings on CD-ROM).

Kocaman, S., Gruen, A., 2007. Rigorous Sensor Modeling of ALOS/PRISM Imagery. 8th Conference on Optical 3D Measurement Techniques, Zurich, Switzerland, 9-12 July.

Kocaman, S., Wolff, K., Gruen, A., Baltsavias, E., 2008. Geometric validation of Cartosat-1 imagery. International Archives of Photogrammetry and Remote Sensing. In press.

Krishnaswamy, M., 2002. Sensors and Platforms for High Resolution Imaging for Large Scale Mapping Applications - Indian Scenario. Indian Cartographer, DAPI-01, URL: http://www.incaindia.org/technicalpapers/02_DAPI01.pdf (accssed 9 May 2008).

Poli, D., 2005. *Modelling of Spaceborne Linear Array Sensors.* Doctoral Thesis. IGP Mitteilungen Nr.85, ISSN 0252-9335 ISBN 3-906467-50-3.